CrystEngComm

Accepted Manuscript

ROYAL SOCIETY OF CHEMISTRY

www.rsc.org/crystengcomm

Cite this: DOI: 10.1039/c0xx00000x

www.rsc.org/xxxxxx

ARTICLE TYPE

Mn(II) Coordination Polymers Assembled from 8 or 9-Connected Trinuclear Secondary Building Units: Topology Analysis and Research of Magnetic Properties

Lu Liu[a], Xiaofeng Lv[a], Lin Zhang[a], Li'an Guo[a], Jie Wu*[a], Hongwei Hou*[a], Yaoting Fan[a]

Received (in XXX, XXX) Xth XXXXXXXXX 20XX, Accepted Xth XXXXXXXXX 20XX
First published on the web Xth XXXXXXXXX 20XX
DOI: 10.1039/b000000x

Two new Mn(II) coordination polymers, namely, $\{[Mn_3L_2(pbbm)]\cdot CH_3CN\}_n$ (**1**) and $[Mn_3L_2(CH_3CN)_2]_n$ (**2**) (pbbm = 1,1'-(1,5-pentane)bis-benzimidazole) have been prepared by engaging a 3,4-bi(4-carboxyphenyl)-benzoic acid (H_3L) ligand under solvothermal conditions. Single-crystal X-ray diffraction studies indicate that **1** and **2** are all three-dimensional frameworks fabricated by trinuclear Mn(II) subunits. Topological analysis manifests that **1** is a 3-nodal (3,4,9)-connected new topology with the Schläfli symbol of $(3\cdot4^2)(3\cdot4^2\cdot6^3)$ $(3^4\cdot4^6\cdot5^6\cdot6^{14}\cdot7^6)$; while **2** is a 4,8-c *flu* network topology with the Schläfli symbol of $(4^6)(4^{12}\cdot6^{12}\cdot8^4)$. **1** and **2** possess excellent chemical resistance to boiling water and organic solvents. The variable temperature magnetization measurements ($\chi_M T$-T and χ_M^{-1}-T) make clear that both of the complexes display ferrimagnetic interactions at the low-temperature region. The value of field-dependent magnetization measurements *M(H)* does not reach the clear saturation values because of magnetic anisotropy of the polycrystalline sample. By the alternating-current (AC) susceptibility measurements, the frequency-dependent peaks do not appear in all of in-phase (χ') and out-of-phase (χ'') curves, indicating that there is no slow relaxation behavior of the magnetization. Markedly, the field-cooled (FC) and zero-field-cooled (ZFC) data of **1** display the divergence over the temperature range 40−3.5 K, which could be on account of the presence of long-range magnetic ordering, or the impact of superparamagnetic behavior. Specially, **2** is based on a typical $-J_1J_1J_2-$ sequence, featuring the ferrimagnetic chain of a (5/2, 10/2) spin topology.

Introduction

In recent years, an upsurge of attention has been paid to the construction of magnetic metal−organic frameworks (MOFs) because they display fascinating structures/topologies and magnetic properties synchronously.[1-3] The investigation of magnetic MOFs may be in favor of comprehending the magneto-structural corelations, and will also furnish an efficient platform for further development of novel functional magnetic materials.[4] Most of magnetic materials are accomplished in bottom-up methods by connecting the paramagnetic transition-metal ions (spin carriers) through multidentate bridging ligands (bridges).[5-6] The reciprocity between the magnetic nature of the spin carrier (distorted coordination environments and single-ion anisotropy) and the superexchange interaction by bridging magnetic bridges affects the magnetism of the entity in a certain extent, which are tanglesome and hard to predict.[7] Therefore, the reasonable design and synthesis of new molecular magnets is still a formidable challenge. The bridging ligands invariably play a key role in the construction of molecular magnets, since they can act as efficient superexchange pathways to convey various magnetic information among the spin carriers.[6h] Averagely, the shorter and more conjugated bridges will lead to the more favorable magnetic coupling transmission between two spins.[8] However, shorter bridges are slightly lacking on the multiformity of bridging modes.[9] Acknowledged polycarboxylic bridges owning abundant coordination modes are well-suited candidates to fabricate

[a] *The College of Chemistry and Molecular Engineering, Zhengzhou University, Zhengzhou 450052, P. R. China* Fax: (+86) 371– 67761744 *E-mail: houhongw@zzu.edu.cn* *†Electronic supplementary information (ESI) available: selected bond lengths and bond angles, powder X-ray patterns, TGA curves for complexes **1** and **2**, molecular structures of free ligand. CCDC reference numbers: 996998–996999 for **1** and **2**. For ESI and crystallographic data in CIF or other electronic format see DOI:10.1039/b000000x/*

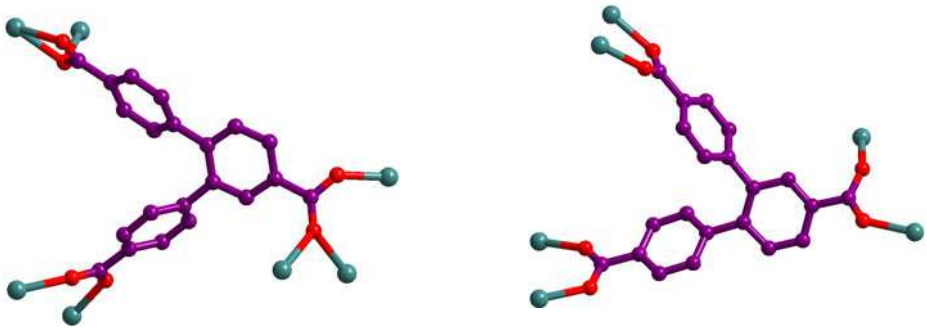

Mode I Mode II

Chart 1. Different Coordination Modes of H_3L in Complexes **1** and **2**

molecular magnets. They are able to not only transmit the magnetic coupling interactions to varying degrees,[10] but also aggregate metal ions into metal clusters (as secondary building units) with specific coordination geometry[11] and extend the metal clusters into aesthetically enjoyable frameworks with exquisite structural topologies.[12]

These metal clusters as SBUs are very significant for the understanding of the magnetism of MOFs. As the metal clusters increase in size, MOFs would display surprising magnetic properties. Besides, the applications of SBUs have also been recommended involving the field of quantum computing[13] and memory devices[14]. It is a pity that the creation of expected SBUs, particularly high-connected SBUs, is proved to be difficult, considering these SBUs always in situ generated discretionarily.[15] Thus, we purposefully choose an asymmetric tripodal multicarboxylic ligand 3,4-bi(4-carboxyphenyl)-benzoic acid (H_3L) (as shown in Scheme S1) as bridges to construct high-connected clusters-based magnetic architectures. The conjugated H_3L ligand possesses important superiorities due to the rigid multicarboxylic groups and consequent tendency to be completely or partially deprotonated, and these anions exhibiting different coordination modes may serve as bridging ligands to generate polynuclear clusters and also can propagate better magnetic superexchange between metal ions. From the viewpoint of property investigation, the magnetic 3d transition metal ions, such as Mn(II), Cu(II), Fe(II), Co(II) and Ni(II) can offer good opportunities for the magnetic investigation, both experimentally and theoretically.[16] Herein, we have mainly focused on Mn(II) ion as the paramagnetic center for two reasons: first, the high-spin Mn(II) includes up to five unpaired electrons, and the combination of Mn(II) with polycarboxylate is inclined to the formation of larger SBUs and stretched solids, such as Mn2, Mn3, Mn4 and Mn−OCO−Mn chain;[17] second, Mn(II) clusters always display large, and sometimes more larger spin (S) values in the ground state, and S is combined with a large anisotropy, perhaps leading some of these species to be single-molecule magnets (SMMs).[18-19]

In this article, we have succeeded in obtaining single crystals of two high-connected trinuclear Mn(II)-clusters molecular magnetism $\{[Mn_3L_2(pbbm)]\cdot CH_3CN\}_n$ (**1**) and $[Mn_3L_2(CH_3CN)_2]_n$ (**2**) (pbbm = 1,1'-(1,5-pentane)bis-benzimidazole) by employing a H_3L ligand to self-assemble with Mn(II) under solvothermal conditions. The solvent resistance property and thermal stability have been investigated. Their variable temperature magnetization measurements ($\chi_M T$-T and χ_M^{-1}-T), field-dependent magnetization measurements $M(H)$, field-cooled and zero-field-cooled magnetization measurements (FC-ZFC) and alternating-current (AC) susceptibility measurements have also been detailedly inquiried and deeply discussed. Both of them exhibit ferromagnetic behaviour at the low-temperature region. The FC and ZFC data of **1** embodies the divergence over the temperature range 40−3.5 K. **2** features the ferrimagnetic chain of a (5/2, 10/2) spin topology.

Experimental section

Materials and Physical Measurements.

All of materials were commercially improvable without any further purification. The ligand pbbm were synthesized according to the literature.[20] The FT-IR spectra of samples were carried out with KBr pellets and achieved in the region of 400−4000 cm^{-1} using a Bruker-ALPHA spectrophotometer. Elemental analyses of C, H, and N were calendared on a FLASH EA 1112 elemental analyzer. All the PXRD patterns were recorded on a PANalytical X'Pert PRO diffractometer with the use of Cu $K\alpha_1$ radiation. Thermal analyses of samples were executed adopting a Netzsch STA 449C thermal analyzer with a heating rate of 10 ºC min^{-1} from ambient temperature under an air atmosphere.

Synthesis

Synthesis of $\{[Mn_3L_2(pbbm)]\cdot CH_3CN\}_n$ (1). A mixture of $MnCl_2\cdot 4H_2O$ (0.0197 g, 0.1 mmol), L (0.0181 g, 0.05 mmol), pbbm (0.0152 g, 0.05 mmol) (pbbm = 1,1'-(1,5-pentane)bis-benzimidazole), CH_3CN (7 mL) and H_2O (3 mL) was heated at 160 °C for three days in a 25 mL Teflon-lined stainless steel vessel. After the mixture was cooled, colourless leaf-shaped crystals suitable for X-ray diffraction were separated, then washed with mother solution, and air-dried (yield, 73% based on Mn). Anal. Calcd for $C_{63}H_{45}Mn_3N_5O_{12}$ (%): C, 61.57; H, 3.69; N, 5.69. Found: C, 61.54; H, 3.71; N, 5.65. IR (KBr, cm^{-1}): 3447(w), 3041(vw), 2924(w), 2863(w), 2249(vm), 1628(m), 1597(m), 1583(m), 1537(m), 1500(w), 1463(w),

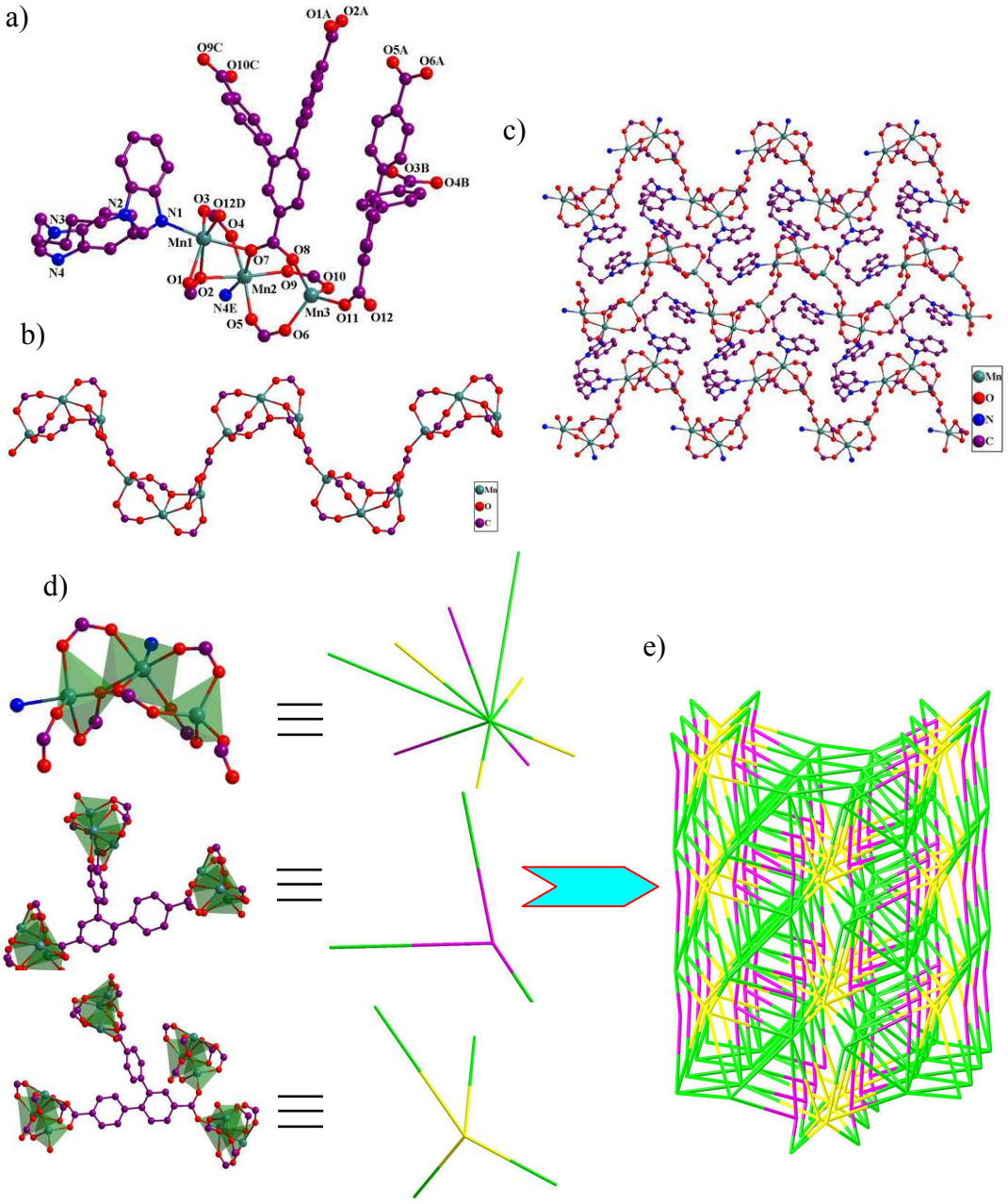

Figure 1. (a) Coordination environment of Mn(II) ion in **1** with hydrogen atoms omitted for clarity. Symmetry code: A = x, −1 + y, z; B = 2 − x, 1 − y, −0.5 + z; C = 2 − x, 1 − y, 0.5 + z; D = 1.5 − x, y, 0.5 + z. (b) The *syn-anti*-μ_2-η^1:η^1 carboxylate bridges (O11−C24−O12) link the trinuclear Mn(II) SBUs into a 1D chain. (c) Schematic diagram of the 2D network accomplished by the 1D chain and pbbm linker. (d) The defined 3-, 4- and 9-connected nodes. (e) Schematic representation of topological net of **1**.

1396(s), 1292(w), 1258(w), 1188(w), 1174(w), 1149(w), 1099(vw), 1014(w), 967(w), 941(w), 921(w), 907(w), 892(w), 871(w), 864(w), 857(w), 847(vw), 799(vw), 782(m), 766(m), 751(m), 742(m), 729(m), 714(m), 681(w), 655(w), 635(w), 610(w), 575(w), 560(w), 515(w), 485(m), 469(m).

Synthesis of $[Mn_3L_2(CH_3CN)_2]_n$ (2). The preparation process of **2** is similar to that of **1**, except that Hatz (Hatz = 1*H*-1,2,4-triazol-3-amine) was used instead of pbbm (0.0042 g, 0.05 mmol). Yield, 59% (based on Mn). Anal. Calcd for $C_{46}H_{28}Mn_3N_2O_{12}$ (%): C, 57.22; H, 2.92; N, 2.90. Found: C, 57.20; H, 2.89; N, 2.93. IR (KBr, cm^{-1}): 3410(m), 2278(w), 1664(w), 1607(m), 1577(m), 1520(m), 1402(s), 1228(w), 1183(m), 1145(w), 1016(m), 1004(m), 929(w), 898(w), 862(m), 838(w), 796(w), 781(m), 730(w), 715(m), 688(w), 569(w), 467(w).

Crystal Data Collection and Refinement.

The collections of crystallographic data of **1** and **2** were performed by using a Rigaku Saturn 724 CCD diffractomer at room temperature (Mo-*K*α, λ = 0.71073 Å). Absorption corrections were accomplished using multi-scan program. The Lorentz and polarization effects were used for correcting the data. The structures were solved by immediate methods and refined based on F^2 with a full-matrix least-squares technique adopting

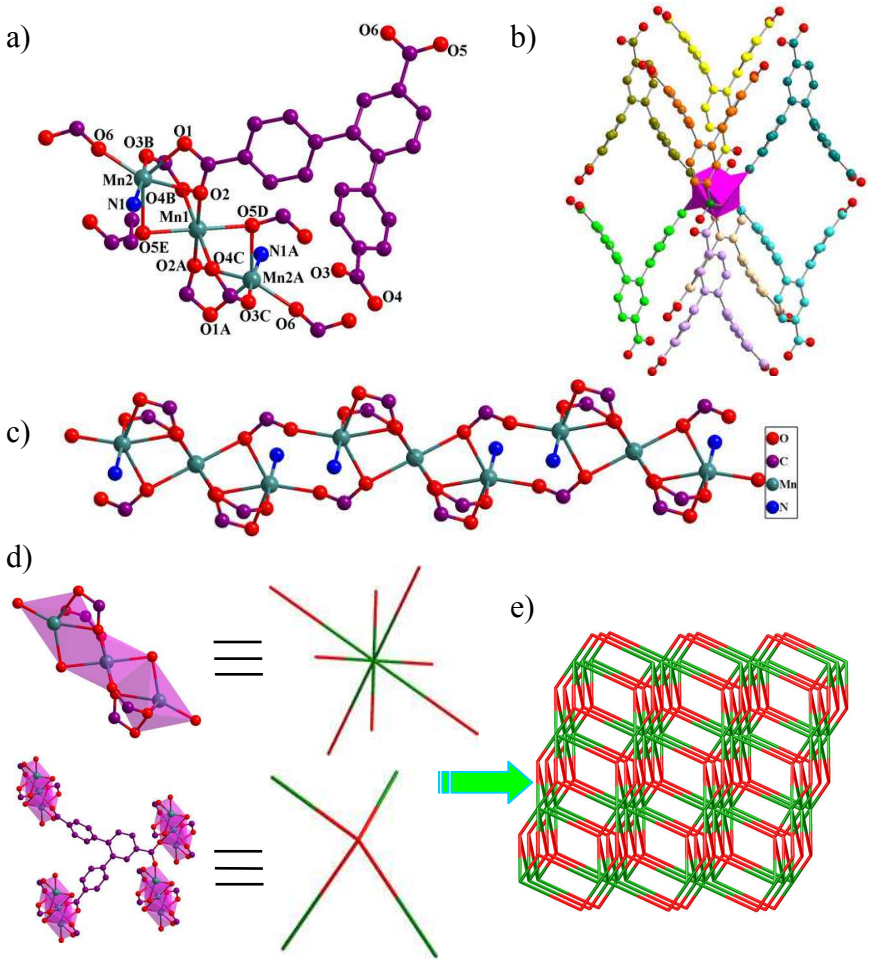

Figure 2. (a) Coordination environment of Mn(II) ion in **2** with hydrogen atoms omitted for clarity. Symmetry code: A = 2 − x, 1 − y, − z; B = 1 + x, −1 + y, z; C = 1 − x, 2 − y, − z; D = 1 − x, 1 − y, 1 − z; E = 1 + x, y, −1 + z. (b) The three-core Mn(II) units links eight L ligands leading to the presence of a beautiful "butterfly" pattern. (c) Perspective view of 1D metal carboxylate chains. (d) The defined 4- and 8-connected nodes. (e) Schematic representation of topological net of **2**.

the SHELXL-97 crystallographic software package.[21] All of the non-hydrogen atoms were refined anisotropically. The hydrogen atoms of ligands were assigned at idealized positions using a riding model and then refined isotropically. Experimental details of the X-ray analyses for **1** and **2** are summarized in Table 1. Selected bond lengths and bond angles of **1** and **2** are listed in Table S1 in the Supporting Information. Crystallographic data for **1** and **2** have been deposited at the Cambridge Crystallographic Data Centre with CCDC reference numbers 996998–996999.

Solvent Resistance Experiment.

The experiment was surveyed by suspending crystal samples in boiling common solvents for 48 h. During this process, the samples were monitored under a SZM45 optical microscope periodically. The refluxed samples were bathed with water and then dried naturally. Single-crystal X-ray diffraction was employed to implement the measurement of the unit-cell parameters.

Magnetic Experiment.

Variable-temperature magnetic susceptibilities were carried out on a SQUID MPMS XL-7 instrument with phase-pure crystalline samples under the applied field of 1 kOe in the temperature region of 2−300 K. The field dependences of magnetization (M) have been performed at 2 K from −80 to 80 kOe. The field-cooled (FC) and zero-field-cooled (ZFC) magnetization measurements were collected in the temperature range 50−2 K under a 20 Oe low field. The alternating-current (AC) magnetic susceptibility were recorded with oscillating frequencies (from 10000 to 10 Hz) at a zero direct-current (DC) field with an AC field of 3 Oe. The diamagnetic corrections were conducted utilizing Pascal's constants.[22]

Results and discussion

Preparation of the Complexes.

Complexes **1** and **2** were prepared from the solvothermal reaction between $MnCl_2 \cdot 4H_2O$ and 3,4-bi(4-carboxyphenyl)-benzoic acid together with secondary ligands in a 2:1:1 molar ratio. The reaction medium was acetonitrile and water (7:3) under 160 ºC. The employment of pbbm (pbbm = 1,1'-(1,5-pentane)bis-benzimidazole) led to the generation of the perfect single crystal **1**. Here, pbbm participated in the coordination with metal ions, resulting in a new nine-connected trinuclear SBUs. When the Hatz (Hatz = 1*H*-1,2,4-triazol-3-amine) was introduced into the

Table 1 Crystallographic data and structure refinement details for complexes 1 and 2[a,b]

Complex	**1**	**2**
formula	$C_{63}H_{45}Mn_3N_5O_{12}$	$C_{46}H_{28}Mn_3N_2O_{12}$
fw	1228.86	965.52
T/K	293(2)	293(2)
λ (Mo K), Å	0.71073	0.71073
Cryst syst	Orthorhombic	Triclinic
Space group	*Pca2₁*	*P-1*
a (Å)	25.926(5)	8.8451(18)
b (Å)	13.837(3)	10.334(2)
c (Å)	15.243(3)	11.762(2)
α(°)	90	77.05(3)
β(°)	90	81.50(3)
γ(°)	90	75.82(3)
V (Å^3)	5468.4(19)	1011.0(4)
Z	4	1
$D_{calcd.}$(g·cm^{-3})	1.493	1.586
abs coeff/mm^{-1}	0.753	0.993
F(000)	2516	489
θ (°)	2.06-25.50	1.79-25.00
GOF	1.001	0.995
R_1(I>2sigma(I))[a]	0.0885	0.0510
wR_2(I>2sigma(I))[b]	0.1574	0.1210

[a] $R_1 = \sum||F_o|-|F_c||/\sum|F_o|$. [b] $wR_2 = [\sum w(F_o^2-F_c^2)^2/\sum w(F_o^2)^2]^{1/2}$.

synthetic system, the transparent crystal of **2** can be obtained, displaying an eight-connected trinuclear SBUs. The architectural differences of **1** and **2** will be exactly discussed below.

Crystal Structure of {[Mn_3L_2(pbbm)]·CH_3CN}$_n$ (1).

Crystal structure determination reveals that **1** crystallizes in orthorhombic space group *Pca*2(1). The asymmetric unit of **1** contains three crystallographically independent Mn^{II} atoms, two completely deprotonated L^{3-} ligands, one pbbm ligand and one guest CH_3CN molecule in the lattice. As illustrated in Figure 1a, Mn1 ion is in a six-coordinated mode (MnO_5N), in which Mn1 is equatorially bonded to carboxylic oxygen atoms (O1, O2, O3 and O12D) from three different L^{3-} ligands (Mn1−O1 = 2.299(6), Mn1−O2 = 2.306(6), Mn1−O3 = 2.124(6), Mn1−O12D = 2.067(6) Å). The two axial sites on the metal are occupied by one N atom from one pbbm ligand (Mn1−N1 = 2.228(7) Å), and one carboxyl O from one L^{3-} ligand (Mn1−O7 = 2.298(6) Å). Mn2 is also has a six-coordinated geormetry MnO_5N, with five carboxyl O atoms from five different L^{3-} ligands (Mn2−O2 = 2.223(6), Mn2−O4 = 2.127(6), Mn2−O5 = 2.145(6), Mn2−O7 = 2.279(6), Mn2−O9 = 2.095(6) Å), and one N atom from one pbbm ligand (Mn2−N4E = 2.268(8) Å). Contrary to Mn1 and Mn2, Mn3 atom is four-coordinated by four oxygen atoms (O6, O8, O10 and O11) from four L^{3-} ligands (Mn3−O6 = 2.025(6), Mn3−O8 = 2.028(6), Mn3−O10 = 2.043(7), Mn3−O11 = 2.009(6) Å), showing a slightly distorted tetrahedral geometry ($\tau_4 \approx 0.94$).[23]

The H_3L in **1** are completely deprotonated, exhibiting two interesting coordination modes: (κ^2-κ^1)-(κ^1-κ^1)-(κ^1-κ^1-μ_3)-μ_7 (Mode I) and (κ^1-κ^1)-(κ^1-κ^1)-(κ^1-κ^1)-μ_6 (Mode II), as shown in Chart 1. In the first mode, three carboxylic groups act as μ_2-η^2:η^1, μ_3-η^2:η^1, and *syn-syn*-μ_2-η^1:η^1 modes in a clockwise direction to

Table 2. The unit-cell parameters of complexes 1 and 2 under specific conditions

		H_2O	MeOH	EtOH	MeCN	DMF
Complex **1**	a (Å)	13.85	13.82	13.82	13.80	13.77
	b (Å)	15.25	15.23	15.20	15.22	15.36
	c (Å)	25.92	25.89	25.86	25.91	25.92
	α (°)	90	90	90	90	90
	β (°)	90	90	90	90	90
	γ (°)	90	90	90	90	90
	V ($Å^3$)	5473	5450	5433	5443	5485
Complex **2**	a (Å)	8.85	8.82	8.89	8.87	8.87
	b (Å)	10.36	10.33	10.41	10.44	10.33
	c (Å)	11.76	11.75	11.84	11.80	11.75
	α (°)	77.33	77.28	77.23	77.36	77.19
	β (°)	81.66	81.61	81.56	81.77	81.63
	γ (°)	75.94	75.90	75.95	76.00	75.77
	V ($Å^3$)	1017	1008	1031	1029	1013

bridge seven Mn(II) ions, severally. In the second mode, three carboxylic groups serve as *syn-syn*-μ_2-η^1:η^1, *syn-anti*-μ_2-η^1:η^1, and *syn-syn*-μ_2-η^1:η^1 modes in a clockwise direction, singly, to bridge six Mn(II) ions. On the basis of these connection modes, Mn1 is linked to Mn2 via three carboxylate groups with the Mn1···Mn2 distance of 3.443 Å, Meanwhile, Mn2 is connected to Mn3 via three carboxylate groups with a Mn2···Mn3 separation of 3.867 Å, thus forming a trinuclear Mn cluster (sea green polyhedron). The trinuclear Mn SBUs are further connected through *syn-anti*-μ_2-η^1:η^1 carboxylate bridges (O11−C24−O12) and assembled into a 1D chain (Figure 1b). These 1D chains are stitched to each other by pbbm with two different $N_{donor}\cdots N\text{-}C_{sp3}\cdots C_{sp3}$ torsion angles of 78.565º and 94.576º, resulting in infinite 2D nets (Figure 1c), which are further linked by L^{3-} with coordination mode I and II to construct a 3D framework.

At the sight of topology, the trinuclear SBU can be defined as a nine-connected node, connecting with seven L^{3-} anions and two pbbm ligands. The L^{3-} ligands in mode I link three trinuclear SBUs, while the L^{3-} ligand in mode II link four trinuclear SBUs. Thus, the L^{3-} ligands in mode I and II are considered as 3-connected nodes and 4-connected nodes, singly (Figure 1d). The final 3D framework exhibits a 3-nodal (3,4,9)-connected topology with the Schläfli symbol of $(3\cdot4^2)(3\cdot4^2\cdot6^3)(3^4\cdot4^6\cdot5^6\cdot6^{14}\cdot7^6)$, which is a new topology (Figure 1e).

Crystal Structure of $[Mn_3L_2(CH_3CN)_2]_n$ (2).

Single-crystal X-ray structural analysis reveals that **2** crystallizes in the triclinic system with $P\bar{1}$ space group. As depicted in Figure 2a, the asymmetric unit contains two crystallographically independent manganese atoms, two completely deprotonated L^{3-} ligands, and two coordinated CH_3CN molecules. The Mn1 center adopts a distorted octahedral geometry, which is completed by four oxygen atoms from four different L^{3-} ligands (O2, O2A, O4B, and O4C) composing the equatorial plane, and two oxygen atoms from two different L^{3-} ligands (O5D and O5E) at the axial positions. The bond angles around Mn1 range from 78.67(11) to 180.00(13)°, and the Mn1−O bond lengths range from 2.133(3) to 2.270(3) Å. Mn2 also adopts a distorted octahedral coordination geometry, but which is coordinated by five carboxylic oxygen atoms (O1, O2, O3B, O5E, and O6) from four different L^{3-} ligands, one nitrogen atom (N1) from one coordinated CH_3CN molecule. The axial positions are filled with O3B and N1 with an O3B−Mn2−N1 bond angle of 173.47(18)°. The Mn2−O/N coordination bond distances range from 2.067(3) to 2.269(3) Å.

In **2**, the L ligand has one coordination mode (Mode I of Chart 1: (κ^2-κ^1)-(κ^1-κ^1)-(κ^1-κ^1-μ_3)-μ_7) to coordinate with Mn^{2+} cations through six carboxyl oxygen atoms, in which three carboxyl groups adopt μ_2-η^2:η^1-chelate/bridge, *syn-syn*-μ_2-η^1:η^1-bridge, and μ_3-η^2:η^1-bridge coordination modes, severally. Mn1 and Mn2 are interconnected by carboxyl groups to form a $Mn_{1.5}$ unit, which further links its symmetric part Mn2A (A = 2−x, 1−y, −z) through the L ligands to furnish a three-core Mn unit (pink polyhedron). The Mn-Mn distance of 3.303 Å is noticeably shorter than that in the carboxylate-bridged trinuclear Mn(II) subunits.[24] The three-core Mn units are connected by bridges of carboxyl groups (O5−C11−O6) to give rise to metal carboxylate chains with the

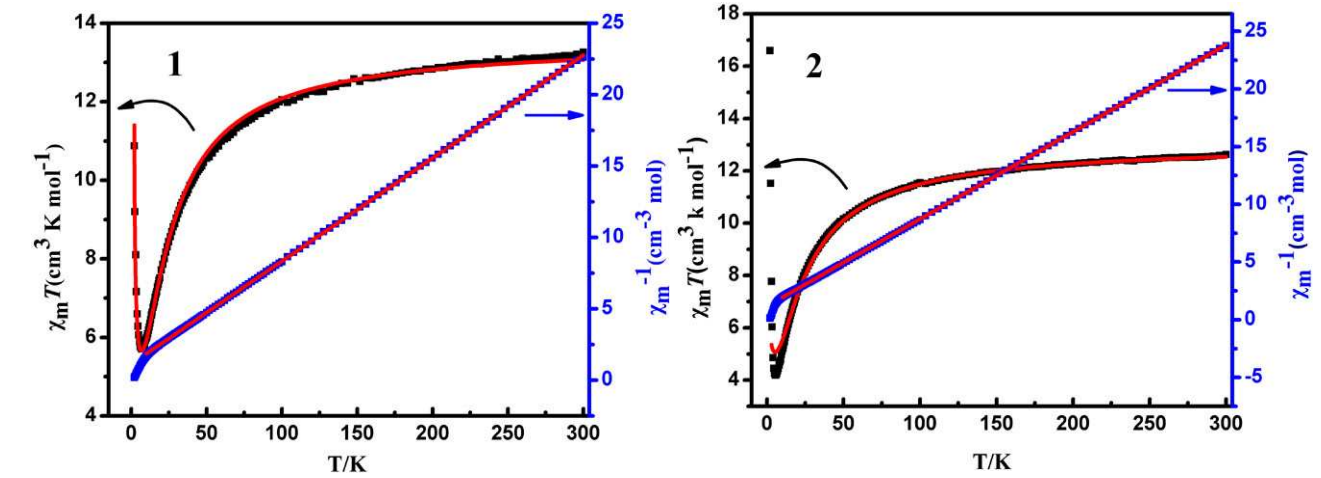

Figure 3. The $\chi_M T$ *vs* T plot and χ_M^{-1} *vs* T plot for polymers **1** and **2** at H = 1 kOe from 2 to 300 K.

terminal CH_3CN molecules (Figure 2c). The metal carboxylate chains are further bridged by L ligands to yield a 3D framework. Furthermore, topological analysis is carried out to get insight of the structure of **2**. The three-core Mn unit links eight L ligands, which leads to the presence of a beautiful "butterfly" pattern (Figure 2b). Thereby, the three-core Mn units can be regarded as 8-connected nodes. Each L^{3-} ligand links four three-core Mn units. Hence, all crystallographical independent L^{3-} ligands act as 4-connected linkers (Figure 2d). As a result, the whole structure can be represented as a 4,8-c *flu* topology network (with the Schläfli symbol $(4^6)(4^{12}\cdot6^{12}\cdot8^4)$) (Figure 2e).

Analyses of Thermal Stability.

The TG analysis of complexes **1** and **2** was performed in the temperature range of 30−800 °C under air atmosphere, and their TG curves are exhibited in Figure S2 (Supporting Information). For **1**, the first step mass loss of 3.20% from 145 to 384 °C could be associated with the release of one guest CH_3CN molecule (calcd 3.34%). The second weight loss from 384 to 512 °C corresponds to the losses of pbbm and L^{3-}. The TG curve of **2** shows the mass loss of 8.01% from 160 to 368 °C, which may be due to the release of two coordinated CH_3CN molecule (calcd 8.49%). The weight loss occurring between 388 and 513 °C could be assigned to the decomposition of the organic ligands.

Analyses of Solvent Resistance Property.

By imitating representative industrial chemical processes, the chemical resistance of complexes **1** and **2** was inquiried by suspending samples in boiling acetonitrile, ethanol, methanol, water and DMF for 48 h. During this process, samples were observed under an optical microscope in cycles. We found that both of them could maintain their original shapes in all the aforementioned solvents. Single-crystal X-ray diffraction indicated that their unit-cell parameters almost did not change (Table 2). Clearly, their primary frameworks were intact and impervious. The outstanding chemical resistance of the two high-connected complexes in refluxing water and frequently-used organic solvents may be attributed to the following reasons. First of all, three benzene rings in the organic linker H_3L can better support the space to present the rigid character, which is likely to be an important factor affecting their chemical stability. Next, the existence of trinuclear Mn(II) clusters as nodes of the entire network could be in favour of the stability of the skeletons. Finally, high connectivity of the clusters give rise to their dense structures, which would also prevent the decomposition of the framework.

Magnetic Properties Measurements.

The magnetic susceptibility measurements on a powdered crystalline sample of complexes **1** and **2** have been conducted in the range of 2−300 K at the applied field of 1 kOe and the magnetic behaviors are displayed in Figure 3. At 300 K, the $\chi_M T$ values of **1** and **2** are 13.14 and 12.58 cm^3 K mol^{-1}, respectively, consistent with the spin-only value as anticipated for three isolated Mn^{2+} ions (13.125 cm^3 mol^{-1} K with S = 5/2) with g = 2.0 per formula unit. The temperature dependence of the reciprocal molar magnetic susceptibility data ($1/\chi_M$) as a function of temperature is linear (above 10 K for **1**; above 20 K for **2**), obeying the Curie−Weiss law of $1/\chi_M = (T - \theta)/C$ with the Curie constant C = 13.86 cm^3 mol^{-1} K and the Weiss constant θ = −15.67 K over the temperature range 10−300 K for **1**, and C = 13.23 cm^3 mol^{-1} K and θ = −15.58 K over the temperature range 20−300 K for **2**, respectively.

Their curves of $\chi_M T$ versus T exhibit analogous diversification in the high-temperature range. As the temperature is lowered, their $\chi_M T$ value slowly decreases and then falls more quickly under 50 K reaching a minimum value of 5.70 cm^3 mol^{-1} K at 7 K for **1** and 4.19 cm^3 mol^{-1} K at 5.5 K for **2**, singly, which demonstrates dominant intramolecular antiferromagnetic interactions among the Mn^{2+} ions. The $\chi_M T$ rises abruptly to 10.88 cm^3 mol^{-1} K for **1** and 16.59 cm^3 mol^{-1} K for **2** at 2 K, which is probably because of ferrimagnetic behavior or spin-canting response that develops into a long-range ordering.

Careful inspection on the crystal structure of **1**, the three main magnetic exchange pathways between neighboring trimeric Mn(II) ions for **1** have been found. One comprises one *syn–syn* carboxyl bridge (Mn-OCO-Mn) and one μ_2-$O_{carboxyl}$ bridge with the exchange angle Mn-$O_{carboxyl}$-Mn of 98.919º between Mn1 and Mn2 (J_{12}). The other is consist of two *syn–syn* carboxyl bridges (Mn-OCO-Mn) between Mn2 and Mn3 (J_{23}). The third one is made up of one *syn–anti* carboxylate bridge (from one μ_3-η^2:η^1-carboxylate group) (J_{13}). There are also possible magnetic

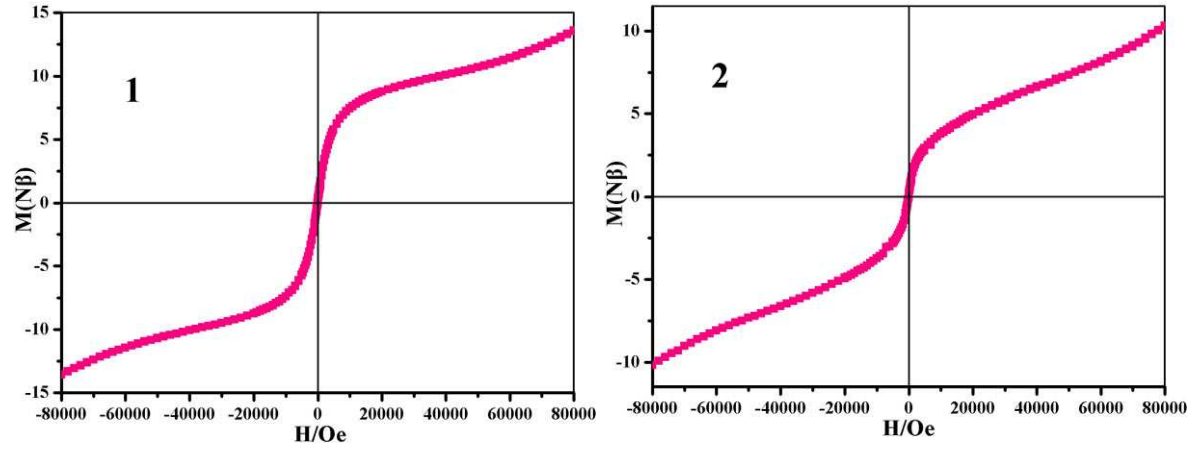

Figure 4. The field-dependent isothermal magnetization for polymers **1** and **2** at 2 K.

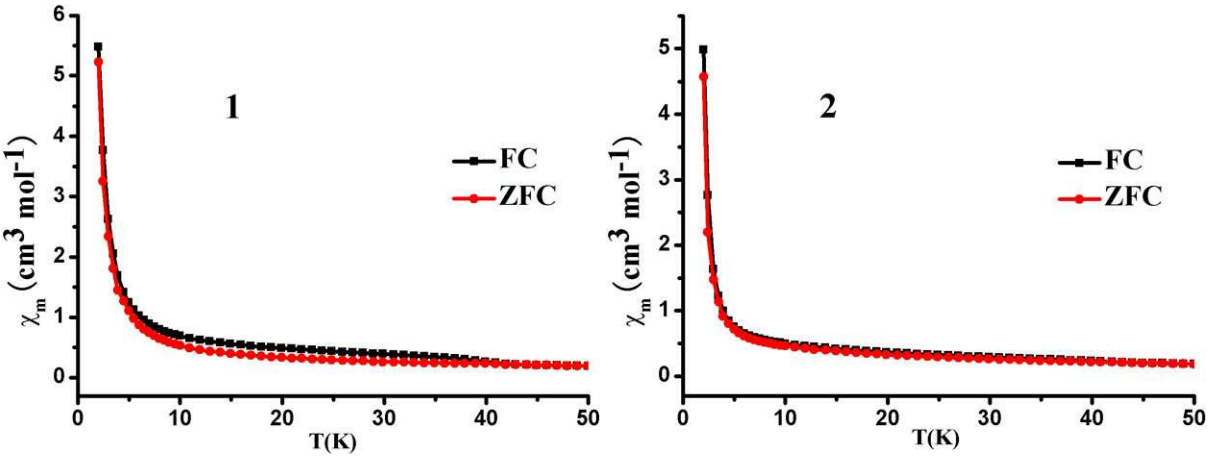

Figure 5. ZFC & FC curves at H = 20 Oe for polymers **1** and **2** from 2 to 50 K.

pathways between trimeric units through the *syn–anti* carboxyl ligand bridges (O12-C24-O11) with a Mn(II)···Mn(II) distance of 5.171 Å, which could be very weak. The magnetic susceptibility data of **1** can be fitted to a trinuclear-Mn(II) model. The Hamiltonian describing the plight of the trimer is given as $\hat{H} = -2J_{12}\hat{S}_1\cdot\hat{S}_2 - 2J_{23}\hat{S}_2\cdot\hat{S}_3 - 2J_{13}\hat{S}_1\cdot\hat{S}_3$. To simplify the calculation, we suppose that the exchange coupling within the cluster is $J_{12} = J_{23} = J_1$, $J_{13} = J_2$. The expression of magnetic susceptibility, induced from the Hamiltonian, is given by:[25]

$$\chi_t = \frac{N\beta^2 g^2}{3kT} \times \frac{\sum_s S_T\left(S_T+1\right)\left(2S_T+1\right)e^{-E(S_T)/kT}}{\sum_S \left(2S_T+1\right)e^{-E(S_T)/kT}}$$

$$\chi_m = \frac{\chi_t}{1-\left(2zJ'/N\beta^2 g^2\right)\chi_t}$$

Best fitting results lead to the following parameters: $g = 2.03$, $J_1 = -1.57$ cm^{-1}, $J_2 = 0.64$ cm^{-1}, $zJ' = 0.14$ K (zJ' stands for the intercluster coupling constants in between trinuclear units) and $R = 1.71\times10^{-4}$, making clear that the results are authentic. (The agreement factor $R = \Sigma[(\chi_M)_{obs} - (\chi_M)_{calac}]^2/\Sigma[(\chi_M)_{obs}]^2$). Distinctly, the negative J_1 value and an antiferromagnetic state were acquired.

From the viewpoint of magnetism, the Mn(II) chains of **2** are parted by the L^{3-} bridges, exhibiting an alternating $-J_1J_1J_2-$ coupling sequence. The magnetic behavior may derive from intra-chain magnetic interactions. According to the chain topology of **2**, there are two sets of magnetic exchange pathways within the chain: one composes of two μ_2-O bridges (from a μ_2-η^2:η^1 and a μ_3-η^2:η^1 carboxylate group, respectively; with the exchange angle Mn-$O_{carboxyl}$-Mn of 94.350º and 96.788º, severally.) between Mn1 and Mn2 and a *syn–syn* carboxylate bridge (J_1); the other is mainly made up of two *syn–anti* carboxylate bridges from two μ_3-η^2:η^1-carboxylate groups (J_2) (Chart S1-above). To obtain noncompensation in spin moments within such a chain, the interaction through the former species of bridges should be antiferromagnetic (AF) and that through the latter species should be ferromagnetic (F), resulting in an AF-AF-F repeating sequence on the basis of a representative (5/2, 10/2) ferrimagnetic chain topology (Chart S1-down).[26]

In order to quantitatively evaluate intra-chain magnetic interactions of **2**, a best fit of the observed magnetic data based on the theoretical expression proposed by Escuer et al.[27] was performed. The fits over the temperature 3–300 K range lead to

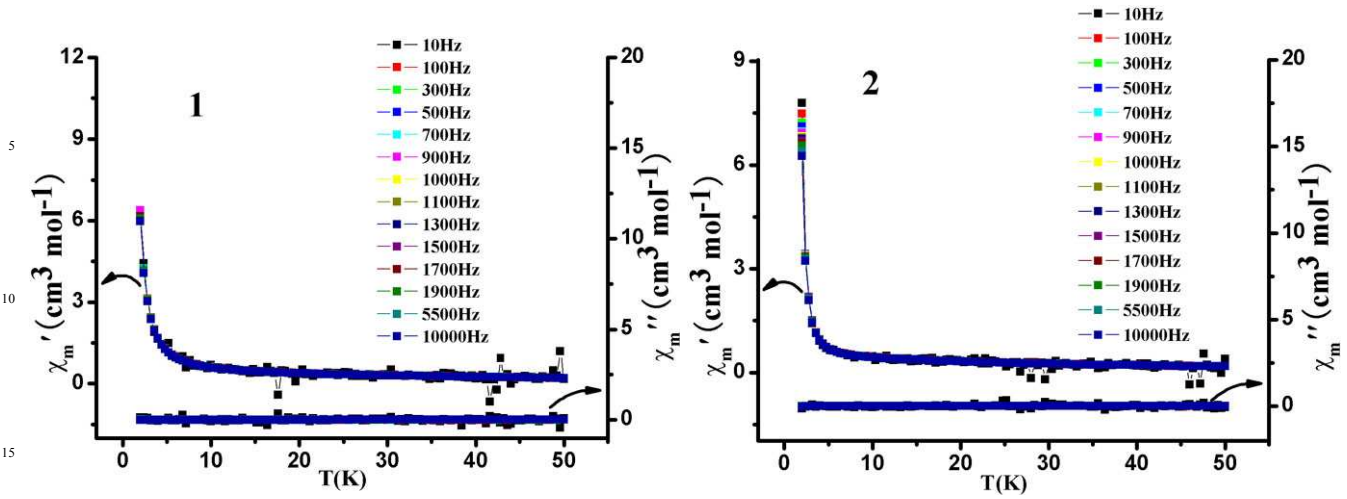

Figure 6. The in-phase χ' and out-of-phase χ'' components of the AC susceptibility of **1** and **2** measured at different frequencies (10, 100, 300, 500, 700, 900, 1000, 1100, 1300, 1500, 1700, 1900, 5500, 10000 Hz) in an applied AC field of 3 Oe.

the following satisfactory parameters for **2**: J_1 = -2.33 cm^{-1}, J_2 = 0.08 cm^{-1}, g = 1.99 and $R = 9.59\times10^{-4}$. The negative J_1 value has correlation with antiferromagnetic (AF) exchange between Mn(II) ions through μ_2-O bridges/*syn–syn* carboxylate bridges, which corresponds to the reported Mn(II) complexes with the same bridging modes.[28] The positive J_2 value is related with weaker ferromagnetic (F) interaction through the dual *syn–anti* bridges, which could be on account of the unexpected orthogonality between magnetic orbitals in the surrounding of Mn(II) ions.[27b]

The magnetic behaviors of the two complexes are further characterized by field-dependent magnetization measurements at 2 K, as their low-temperature magnetizations are distinctly different from each other. As shown in Figure 4, the magnetization curves *M(H)* sharply increase to reach a value of about 9.56 Nβ for **1** and 5.86 Nβ for **2** at a field of 30 kOe, singly. Sudden rise of the curves at the low field signify the presence of ferromagnetic couplings.[29] Then the *M(H)* curves slowly increases to a value of 13.40 Nβ for **1** and 10.20 Nβ for **2** at 80 kOe, respectively, but does not reach the clear saturation values. In addition, the *M* value at the highest field of 80 kOe is not in line with the value expected for a net spin value of S = 5/2 with g = 2.0 (3 × 5.00 Nβ) for three isolated Mn(II) ions. The situation of the *M* vs *H* plot at the high field may be due to the significant magnetic anisotropy of the polycrystalline sample and/or possible low-lying excited states in the complex system[30]. No hysteresis loop in **1** and **2** was observed upon cycling of the field between − 80 and 80 kOe at low temperature, typical of a soft magnet.[31]

The field-cooled (FC) and zero-field-cooled (ZFC) magnetization measurements were performed in the temperature range 50−2 K under a low field (H = 20 Oe) (Figure 5). The FC and ZFC data of **1** display the divergence over the temperature range 40−3.5 K, but the magnetization (χ_M) increases continuously with decreasing temperature and no maximum was observed. The branch of the FC and ZFC data of **1** could be due to the presence of long-range magnetic ordering or superparamagnetic behavior.[32] However, there is almost no discrepancy in the field-cooled and zero-field-cooled magnetization below 50 K for **2**. The phenomenon manifests the absence of any long-range magnetic ordering.

To further examine the magnetization dynamics, their alternating-current (AC) susceptibility measurements are also carried out in the temperature range 50−2 K under H_{DC} = 0 Oe and H_{AC} = 3 Oe for oscillating frequencies (from 10000 to 10 Hz). As depicted in Figure 6, frequency-dependent peaks did not consistently appear in all of in-phase (χ') and out-of-phase (χ'') curves, revealing that there is no slow relaxation behavior of the magnetization. The results suggest that complexes **1** and **2** are not single-molecule magnets (SMMs).

Magneto-structural Correlation Studies.

The magnetic exchange system in the MOFs is very intricate in nature. Among the super exchange pathways between the adjoining Mn(II) ions, ferro- or antiferromagnetic couplings could happen relying on the versatile carboxylate bridging fashions. A *syn-syn* carboxylate bridging pattern furnishes small metal-metal separations, which will trigger antiferromagnetic coupling between the metal centres.[33] The *syn-anti* carboxylate bridging mode may yield antiferromagnetic or ferromagnetic coupling between metal atoms.[34] Besides, in the light of Goodenough's rules, the μ_2-$O_{carboxyl}$ bridge can mediate ferromagnetic couplings, because the relevant Mn-$O_{carboxyl}$-Mn angles (87.97–100.69º) are within the range anticipated for a ferromagnetic interaction.[31a, 35] In **1**, the existence of Mn-OCO-Mn with the *syn-syn* conformations between Mn1 and Mn2/ Mn2 and Mn3, μ_2-$O_{carboxyl}$ bridge with small exchange angle Mn-$O_{carboxyl}$-Mn of 98.919º and the *syn–anti* carboxylate bridges between Mn1 and Mn3 are verified. Meanwhile, two μ_2-O bridges with the exchange angle Mn-$O_{carboxyl}$-Mn of 94.350º and 96.788º, severally, and a *syn–syn* carboxylate bridge between Mn1 and Mn2 dwell in **2**, presenting a $-J_1J_1J_2-$ sequence. For **1**, the negative J_1 makes it reveal antiferromagnetic interaction. For **2**, the negative value of J_1 and the small positive value of J_2 verify that there is an antiferromagnetic (AF) interaction within the trimers as well as a ferromagnetic (F) interaction among the trimers, namely, an alternating AF-AF-F sequence. The AF interaction occupies one dominating status in **2**, seeing that $|J_{AF}|$ is much larger than $|J_F|$. Additionally, by comparing magnetic behaviors of the above 3D coordination polymers with trimeric SBUs, we find that the magnetic exchange coupling constants is

also consistent with the structural of 3D frameworks, particularly the exchange angles of magnetic exchange pathways and metal···metal distances. Nevertheless, the magnetic exchange angles of **1** and **2** are close to each other. Herien, we only consider the effect of metal···metal distances. The shorter metal···metal distances (**1**: 3.867 and 3.443 Å; **2**: 3.303 Å) within SBUs can both bright about strong antiferromagnetic coupling interactions (**1**: J_1 = - 1.57; **2**: J_1 = -2.33).

Conclusions

To sum up, two high-connected trinuclear Mn(II)-clusters frameworks have been successfully fabricated by adopting H_3L as ligand to self-assemble with Mn(II) under suitable solvothermal conditions. They show different 3D frameworks with elegant topologies. The results demonstrate that the versatile coordination modes of the carboxylate ligands give play to important effect on tuning the structures of final coordination network. **1** and **2** own high thermal stability (up to 384 °C/388 °C) and distinguished chemical resistance in boiling water and common organic solvents. Both of them exhibit ferromagnetic behaviour at the low-temperature region. Their magnetization curves *M(H)* does not reach the clear saturation values, and no hysteresis loop was observed. Nevertheless, the FC and ZFC data of **1** particularly display the divergence over the temperature range 40−3.5 K. More gratifying, **2** features the ferrimagnetic chain of a (5/2, 10/2) spin topology. To some extent, the aforesaid discussion will offer a helpful perspective for the construction of polynuclear complexes and also promote the rapid expansion of magnetic materials. The more systematic work will be done to elucidate the synthetic methods of new types of multinuclear clusters and construct polymers with higher-connected topology and outstanding magnetic properties.

Acknowledgments

This work was financially supported by the National Natural Science Foundation (Nos 21371155 and 21201152) and Research Found for the Doctoral Program of Higher Education of China (20124101110002).

References

1 (a) D. Sarma, P. Mahata, S. Natarajan, P. Panissod, G. Rogez, M. Drillon, *Inorg. Chem.,* 2012, **51**, 4495; (b) D. Zhao, S. Tan, D. Yuan, W. Lu, Y. H. Rezenom, H. Jiang, L. Q. Wang, H. C. Zhou, *Adv. Mater.,* 2011, **23**, 90; (c) M. Ahmad, R. Das, P. Lama, P. Poddar, P. K. Bharadwaj, *Cryst. Growth Des.,* 2012, **12**, 4624; (d) X. Y. Wang, L. Wang, Z. M. Wang, S. Gao, *J. Am. Chem. Soc.,* 2006, **128**, 674.

2 (a) Q. Chen, J. B. Lin, W. Xue, M. H. Zeng, X. M. Chen, *Inorg. Chem.,* 2011, **50**, 2321; (b) E. D. Bloch, D. Britt, C. Lee, C. J. Doonan, F. J. Uribe-Romo, H. Furukawa, J. R. Long, O. M. Yaghi, *J. Am. Chem. Soc.,* 2010, **132**, 14382; (c) G. Férey, *Chem. Soc. Rev.,* 2008, **37**, 191; (d) S. Bureekaew, H. Sato, R. Matsuda, Y. Kubota, R. Hirose, J. Kim, K. Kato, M. Takata, S. Kitagawa, *Angew. Chem. Int. Ed.,* 2010, **49**, 7660; (e) J. Xiao, B. Y. Liu, G. Wei, X. C. Huang, *Inorg. Chem.,* 2011, **50**, 11032; (f) W. Yuan, T. Friščić, D. Apperley, S. L. James, *Angew. Chem. Int. Ed.,* 2010, **49**, 3916; (g) J. P. Zhang, A. X. Zhu, R. B. Lin, X. L. Qi, X. M. Chen, *Adv. Mater.,* 2011, **23**, 1268.

3 (a) P. Kar, R. Haldar, C. J. Gómez-García, A. Ghosh, *Inorg. Chem.,* 2012, **51**, 4265; (b) Z. Guo, H. Wu, G. Srinivas, Y. Zhou, S. Xiang, Z. Chen, Y. Yang, W. Zhou, M. O'Keeffe, B. Chen, *Angew. Chem. Int. Ed.,* 2011, **50**, 3178; (c) W. L. Leong, J. J. Vittal, *Chem. Rev.,* 2011, **111**, 688; (d) Q. Yang, J. P. Zhao, B. W. Hu, X. F. Zhang, X. H. Bu, *Inorg. Chem.,* 2010, **49**, 3746; (e) S. T. Zheng, F. Zuo, T. Wu, B. Irfanoglu, C. Chou, R. A. Nieto, P. Feng, X. Bu, *Angew. Chem. Int. Ed.,* 2011, **50**, 1849; (f) J. J. Perry, J. A. Perman, M. J. Zaworotko, *Chem. Soc. Rev.,* 2009, **38**, 1400; (g) X. M. Zhang, Z. M. Hao, W. X. Zhang, X. M. Chen, *Angew. Chem. Int. Ed.,* 2007, **46**, 3456.

4 F. Yang, B. Y. Li, W. Xu, G. H. Li, Q. Zhou, J. Hua, Z. Shi, S. H. Feng, *Inorg. Chem.,* 2012, **51**, 6813.

5 (a) X. H. Chang, J. H. Qin, L. F. Ma, J. G. Wang, L. Y. Wang, *Cryst. Growth Des.,* 2012, **12**, 4649; (b) G. Y. An, C. M. Ji, A. L. Cui, H. Z. Kou, *Inorg. Chem.,* 2011, **50**, 1079; (c) S. N. Zhao, S. Q. Su, X. Z. Song, M. Zhu, Z. M. Hao, X. Meng, S. Y. Song, H. J. Zhang, *Cryst. Growth Des.,* 2013, **13**, 2756; (d) F. C. Liu, M. Xue, H. C. Wang, J. Ou-Yang, *Eur. J. Inorg. Chem.,* 2010, 4444; (e) Q. Gao, F. L. Jiang, M. Y. Wu, Y. G. Huang, W. Wei, M. C. Hong, *Cryst. Growth Des.,* 2010, **10**, 184; (f) P. P. Yang, H. B. Song, X. F. Gao, L. C. Li, D. Z. Liao, *Cryst. Growth Des.,* 2009, **9**, 4064; (g) S. Wöhlert, M. Wriedt, T. Fic, Z. Tomkowicz, W. Haase, C. Näther, *Inorg. Chem.,* 2013, **52**, 1061.

6 (a) J. Olguín, M. Kalisz, R. Clérac, S. Brooker, *Inorg. Chem.,* 2012, **51**, 5058; (b) L. Hou, B. Liu, L. N. Jia, L. Wei, Y. Y. Wang, Q. Z. Shi, *Cryst. Growth Des.,* 2013, **13**, 701; (c) S. Mukherjee, D. Samanta, P. S. Mukherjee, *Cryst. Growth Des.,* 2013, **13**, 5335; (d) K. C. Mondal, Y. Song, P. S. Mukherjee, *Inorg. Chem.,* 2007, **46**, 9736; (e) H. R. Wen, C. F. Wang, Y. Song, S. Gao, J. L. Zuo, X. Z. You, *Inorg. Chem.,* 2006, **45**, 8942; (f) S. Mukherjee, B. Gole, Y. Song, P. S. Mukherjee, *Inorg. Chem.,* 2011, **50**, 3621; (g) D. K. Cao, J. Q. Feng, M. Ren, Y. W. Gu, Y. Song, M. D. Ward, *Chem. Commun.,* 2013, **49**, 8863; (h) E. C. Yang, Z. Y. Liu, X. J. Shi, Q. Q. Liang, X. J. Zhao, *Inorg. Chem.,* 2010, **49**, 7969.

7 E. C. Yang, Z. Y. Liu, X. Y. Wu, H. Chang, E. C. Wang, X. J. Zhao, *Dalton Trans.,* 2011, **40**, 10082.

8 (a) X. Y. Wang, Z. M. Wang, S. Gao, *Chem. Commun.,* 2008, 281; (b) S. Altmannshofter, E. Herdtweck, F. H. Köhler, R. Miller, R. Mölle, E. W. Scheidt, W. Scherer, C. Train, *Chem. Eur. J.,* 2008, **14**, 8013; (c) H. Miyasaka, T. Madanbashi, A. Saitoh, N. Motokawa, R. Ishikawa, M. Yamashita, S. Bahr, W. Wernsdorfer, R. Clérac, *Chem. Eur. J.,* 2012, **18**, 3942; (d) Y. F. Zeng, X. Hu, F. C. Liu, X. H. Bu, *Chem. Soc. Rev.,* 2009, **38**, 469.

9 (a) D. M. Pajerowski, M. J. Andrus, J. E. Gardner, E. S. Knowles, M. W. Meisel, D. R. Talham, *J. Am. Chem. Soc.,* 2010, **132**, 4058; (b) J. Lefebvre, P. Tyagi, S. Trydel, V. Pacradouni, C. Kaiser, J. Sonier, D. B. Leznoff, *Inorg. Chem.,* 2009, **48**, 55.

10 (a) L. M. Duan, F. T. Xie, X. Y. Chen, Y. Chen, Y. K. Lu, P. Cheng, J. Q. Xu, *Cryst. Growth Des.,* 2006, **6**, 1101; (b) T. K. Maji, S. Sain, G. Mostafa, T. H. Lu, J. Ribas, M. Monfort, N. R. Chauhuri, *Inorg. Chem.,* 2003, **42**, 709; (c) N. Guillou, S. Pastre, C. Livage, G. Férey, *Chem. Commun*., 2002, 2358; (d) S. Konar, P. S. Mukherjee, E. Zangrando, F. Lloret, N. R. Chaudhuri, *Angew. Chem. Int. Ed.,* 2002, **41**, 1561; (e) Y. Rodríguez-Martín, M. Hernández-Molina, F. S. Delgado, J. Pasán, C. Ruiz-Pérez, F. Lloret, M. Julve, *CrystEngComm.,* 2002, **4**, 522; (f) T. F. Liu, H. L. Sun, S. Gao, S. W. Zhang, T. C. Lau, *Inorg Chem.,* 2003, **42**, 4792; (g) S. L. Huang, L. H. Weng, G. X. Jin, *Dalton Trans*., 2012, **41**, 11657.

11 (a) B. Chen, N. W. Ockwig, F. R. Fronczek, D. S. Contreras, O. M. Yaghi, *Inorg. Chem.,* 2005, **44**, 181; (b) L. Luo, K. Chen, Q. Liu, Y. Lu, T. Okamura, G. C. Lv, Y. Zhao, W. Y. Sun, *Cryst. Growth Des.,* 2013, **13**, 2312; (c) J. L. C. Rowsell, A. R. Millward, K. S. Park, O. M. Yaghi, *J. Am. Chem. Soc.,* 2004, **126**, 5666; (d) O. M. Yaghi, M. O'keeffe, M. W. Ockwig, H. K. Chae, M. Eddaoudl, J. Kim, *Nature* 2003, **423**, 705; (e) M. Eddaoudi, J. Kim, N. Rosi, D. Vodak, J. Wachter, M. O'Keeffe, O. M. Yaghi, *Science* 2002, **295**, 469.

12 (a) Z. R. Pan, Y. Song, Y. Jiao, Z. J. Fang, Y. Z. Li, H. G. Zheng, *Inorg. Chem.,* 2008, **47**, 5162; (b) C. N. R. Rao, S. Natarajan, R. Vaidhyanathan, *Angew. Chem. Int. Ed.*, 2004, **43**, 1466; (c) C. Janiak, *Dalton Trans.*, 2003, 2781; (d) S. L. James, *Chem. Soc. Rev.*, 2003, **32**, 276; (e) C. S. Lim, J. K. Schnobrich, A. G. Wong-Foy, A. J. Matzger, *Inorg. Chem.,* 2010, **49**, 5271.

13 (a) J. Lehmann, A. Gaita-Arino, E. Coronado, D. Loss, *J. Mater. Chem.,* 2009, **19**, 1672; (b) G. A. Timco, S. Carretta, F. Troiani, F. Tuna, R. J. Pritchard, C. A. Muryn, E. J. L. McInnes, A. Ghirri, A.

Candini, P. Santini, G. Amoretti, M. Affronte, R. E. P. Winpenny, *Nat. Nanotechnol.,* 2009, **4**, 173.
14 (a) M. Cavallini, J. Gomez-Segura, D. Ruiz-Molina, M. Massi, C. Albonetti, C. Rovira, J. Veciana, F. Biscarini, *Angew. Chem. Int. Ed.,* 2005, **117**, 910; *Angew. Chem. Int. Ed.,* 2005, **44**, 888; (b) M. Affronte, *J. Mater. Chem.,* 2009, **19**, 1731.
15 (a) G. E. Kostakis, S. P. Perlepesb, V. A. Blatovc, D. M. Proserpiod, A. K. Powell, *Coord. Chem. Rev.,* 2012, **256**, 1246; (b) S. T. Zheng, J. J. Bu, T. Wu, C. Chou, P. Feng, X. Bu, *Angew. Chem. Int. Ed.,* 2011, **50**, 8858; (c) Q. Chen, W. Xue, J. B. Lin, R. B. Lin, M. H. Zeng, X. M. Chen, *Dalton Trans.,* 2012, **41**, 4199.
16 (a) S. Karasawa, N. Koga, *Inorg. Chem.,* 2011, **50**, 2055; (b) T. C. Stamatatos, D. Foguet-Albiol, S. C. Lee, C. C. Stoumpos, C. P. Raptopoulou, A. Terzis, W. Wernsdorfer, S. O. Hill, S. P. Perlepes, G. Christou, *J. Am. Chem. Soc.,* 2007, **129**, 9484; (c) O. Fabelo, J. Pasán, F. Lloret, M. Julve, C. Ruiz-Pérez, *Inorg. Chem.,* 2008, **47**, 3568; (d) C. I. Yang, S. P. Hung, G. H. Lee, M. Nakano, H. L. Tsai, *Inorg. Chem.,* 2010, **49**, 7617; (e) Q. Chu, Z. Su, J. Fan, T. Okamura, G. C. Lv, G. X. Liu, W. Y. Sun, N. Ueyama, *Cryst. Growth Des.,* 2011, **11**, 3885.
17 (a) L. F. Ma, M. L. Han, J. H. Qin, L. Y. Wang, M. Du, *Inorg. Chem.,* 2012, **51**, 9431; (b) X. M. Zhang, Y. Q. Wang, Y. Song, E. Q. Gao, *Inorg. Chem.,* 2011, **50**, 7284; (c) G. Berggren, P. Huang, L. Eriksson, S. Styring, M. F. Anderlund, A. Thapper, *Dalton Trans.,* 2010, **39**, 11035; (d) X. F. Wang, Y. B. Zhang, W. X. Zhang, W. Xue, H. L. Zhou, X. M. Chen, *CrystEngComm.,* 2011, **13**, 4196; (e) W. X. Chen, G. L. Zhuang, H. X. Zhao, L. S. Long, R. B. Huang, L. S. Zheng, *Dalton Trans.,* 2011, **40**, 10237; (f) C. Lampropoulos, G. Redler, S. Data, K. A. Abboud, S. Hill, G. Christou, *Inorg. Chem.,* 2010, **49**, 1325; (g) Y. Q. Wang, Q. Sun, Q. Yue, A. L. Cheng, Y. Song, E. Q. Gao, *Dalton Trans.,* 2011, **40**, 10966; (h) Y. Li, W. Q. Zou, M. F. Wu, J. D. Lin, F. K. Zheng, Z. F. Liu, S. H. Wang, G. C. Guo, J. S. Huang, *CrystEngComm.,* 2011, **13**, 3868.
18 (a) L. Lecren, O. Roubeau, C. Coulon, Y. G. Li, X. F. Le Goff, W. Wernsdorfer, H. Miyasaka, R. Clérac, *J. Am. Chem. Soc.,* 2005, **127**, 17353; (b) C. Lampropoulos, G. Redler, S. Data, K. A. Abboud, S. Hill, G. Christou, *Inorg. Chem.,* 2010, **49**, 1325; (c) J. Yoo, W. Wernsdorfer, E. C. Yang, M. Nakano, A. L. Rheingold, D. N. Hendrickson, *Inorg. Chem.,* 2005, **44**, 3377; (d) K. C. Mondal, M. G. B. Drew, P. S. Mukherjee, *Inorg. Chem.,* 2007, **46**, 5625; (e) E. K. Brechin, C. Boskovic, W. Wernsdorfer, J. Yoo, A. Yamaguchi, E. C. Sañudo, T. R. Concolino, A. L. Rheingold, H. Ishimoto, D. N. Hendrickson, G. Christou, *J. Am. Chem. Soc.,* 2002, **124**, 9710; (f) H. L. Tsai, C. I. Yang, W. Wernsdorfer, S. H. Huang, S. Y. Jhan, M. H. Liu, G. H. Lee, *Inorg. Chem.,* 2012, **51**, 13171.
19 (a) H. Miyasaka, A. Saitoh, S. Abe, *Coord. Chem. Rev.,* 2007, **251**, 2622; (b) J. Yoo, A. Yamaguchi, M. Nakano, J. Krzystek, W. E. Streib, L. C. Brunel, H. Ishimoto, G. Christou, D. N. Hendrickson, *Inorg. Chem.,* 2001, **40**, 4604; (c) J. S. Costa, L. A. Barrios, G. A. Craig, S. J. Teat, F. Luis, O. Roubeau, M. Evangelisti, A. Camón, G. Aromí, *Chem. Commun.,* 2012, **48**, 1413; (d) C. Boskovic, E. Brechin, W. E. Streib, K. Folting, J. C. Bollinger, D. N. Hendrickson, G. Christou, *J. Am. Chem. Soc.,* 2002, **124**, 3725; (e) K. C. Mondal, Y. Song, P. S. Mukherjee, *Inorg. Chem.,* 2007, **46**, 9736.
20 R. Bronisz, *Inorg. Chem.*, 2005, **44**, 4463.
21 G. M. Sheldrick, *Acta Crystallogr. A.* 2008, **64**, 112.
22 E. König, *Magnetic Properties of Coordination and Organometallic Transition Metal Compounds*; Springer: Berlin, 1966.
23 (a) L. Yang, D. R. Powell, R. P. Houser, *Dalton Trans.,* 2007, 955; (b) X. Z. Song, S. Y. Song, C. Qin, S. Q. Su, S. N. Zhao, M. Zhu, Z. M. Hao, H. J. Zhang, *Cryst. Growth Des.,* 2012, **12**, 253.
24 (a) H. J. Chen, Z. W. Mao, S. Gao, X. M. Chen, *Chem. Commun.,* 2001, 2320; (b) R. L. Rardin, P. Poganiuch, A. Bino, D. P. Goldberg, W. B. Tolman, S. Liu, S. J. Lippard, *J. Am. Chem. Soc.,* 1992, **114**, 5240; (c) V. Tangoulis, D. A. Malamatari, K. Soulti, V. Stergiou, C. P. Raptopoulou, A. Terzis, T. A. Kabanos, D. P. Kessissoglou, *Inorg.Chem.,* 1996, **35**, 4974; (d) G. Fernández, M. Corbella, J. Mahía, M. A. Maestro, *Eur. J. Inorg. Chem.,* 2002, 2502.
25 (a) K. F. Hsu, S. L. Wang, *Inorg. Chem.,* 2000, **39**, 1773; (b) O. Kahn, Molecular Magnetism; VCH Publishers Inc.: New York, 1993; p 211; (c) F. Y. Yi, Z. M. Sun, *Cryst. Growth Des.,* 2012, **12**, 5693.
26 C. B. Tian, Z. Z. He, Z. H. Li, P. Lin, S. W. Du, *CrystEngComm.,* 2011, **13**, 3080.
27 (a) M. A. M. Abu-Youssef, M. Drillon, A. Escuer, M. A. S. Goher, F. A. Mautner, R. Vicente, *Inorg. Chem.,* 2000, **39**, 5022; (b) R. H. Wang, E. Q. Gao, M. C. Hong, S. Gao, J. H. Luo, Z. Z. Lin, L. Han, R. Cao, *Inorg. Chem.,* 2003, **42**, 5486.
28 (a) D. Mandal, P. B. Chatterijee, S. Bhattacharya, K. Y. Choi, R. Clérac, M. Chaudhury, *Inorg. Chem.,* 2009, **48**, 1826; (b) H. Adams, D. E. Fenton, L. R. Cummings, P. E. McHugh, M. Ohba, H. Okawa, H. Sakiyama, T. Shiga, *Inorg. Chim. Acta* 2004, **357**, 3648.
29 M. Zhu, Y. G. Li, Y. Ma, L. C. Li, D. Z. Liao, *Inorg. Chem.,* 2013, **52**, 12326.
30 (a) Y. Z. Zheng, Y. Lan, C. E. Anson, A. K. Powell, *Inorg. Chem.,* 2008, **47**, 10813; (b) S. Kanegawa, M. Maeyama, M. Nakano, N. Koga, *J. Am. Chem. Soc.,* 2008, **130**, 3079; (c) K. Bernot, J. Luzon, L. Bogani, M. Etienne, C. Sangregorio, M. Shanmugam, A. Caneschi, R. Sessoli, D. Gatteschi, *J. Am. Chem. Soc.,* 2009, **131**, 5573; (d) P. H. Lin, T. J. Burchell, R. Clérac, M. Murugesu, *Angew. Chem. Int. Ed.,* 2008, **47**, 8848.
31 (a) Z. M. Wang, B. Zhang, H. Fujiwara, H. Kobayashi, M. Kurmooc, *Chem. Commun.,* 2004, 416; (b) H. J. Chen, Z. W. Mao, S. Gao, X. M. Chen, *Chem. Commun.*, 2001, 2320.
32 N. A. Chernova, Y. N. Song, P. Y. Zavalij, M. S. Whittingham, *PHYSICAL REVIEW B 70*, 2004, **144405**, 1.
33 (a) P. king, R. Clérac, C. E. Anson, C. Coulon, A. K. Powell, *Inorg. Chem.,* 2003, **42**, 3492; (b) E. Colacio, J. M. Domínguez-Vera, M. Ghazi, R. Kivekäs, M. Klinga, J. M. Moreno, *Eur. J. Inorg. Chem.,* 1999, 441.
34 S. J. Retting, R. C. Thompson, J. Trotter, S. Xia, *Inorg. Chem.,* 1999, **38**, 1360.
35 J. B. Goodenough, *Magnetism and the Chemical Bond*, Wiley, New York, 1963.

For Table of Contents Use Only

Mn(II) Coordination Polymers Assembled from 8 or 9-Connected Trinuclear Secondary Building Units: Topology Analysis and Research of Magnetic Properties

Lu Liu, Xiaofeng Lv, Lin Zhang, Li'an Guo, Jie Wu*, Hongwei Hou*, Yaoting Fan

Two high-connected trinuclear Mn(II)-clusters polymers have been successfully fabricated. **1** and **2** possess high thermal stability and extraordinary chemical resistance to boiling water and familiar organic solvents. Their $\chi_M T$-T, χ_M^{-1}-T, $M(H)$ and FC-ZFC measurements as well as the AC susceptibility measurements have been detailedly inquiried and deeply discussed. Strikingly, the FC and ZFC data of **1** embodies the divergence over the temperature range 40−3.5 K. **2** features the ferrimagnetic chain of a (5/2, 10/2) spin topology.

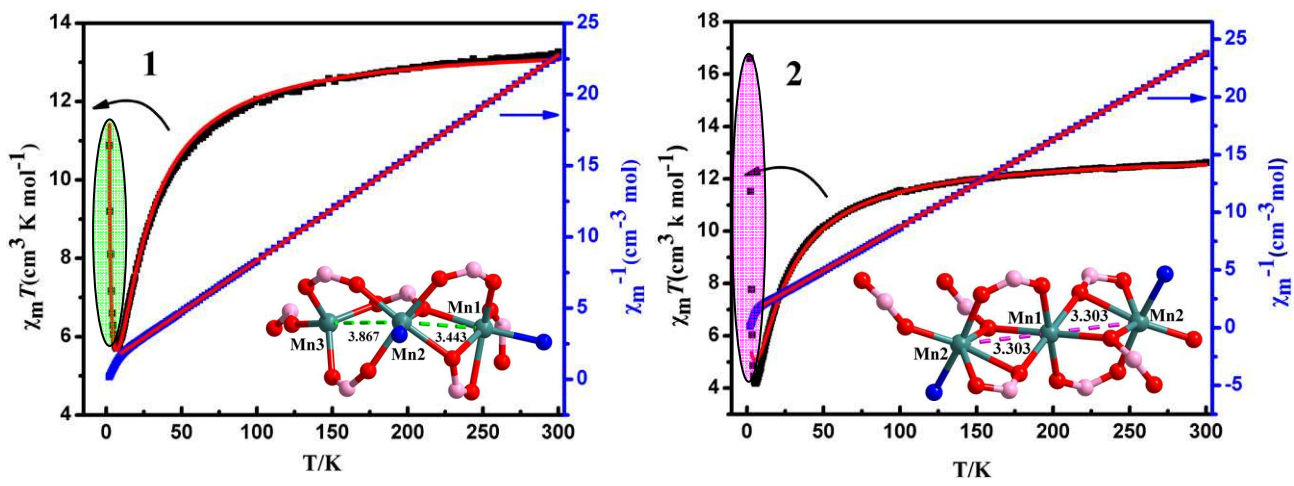

For Table of Contents Use Only

Mn(II) Coordination Polymers Assembled from 8 or 9-Connected Trinuclear Secondary Building Units: Topology Analysis and Research of Magnetic Properties

Lu Liu, Xiaofeng Lv, Lin Zhang, Li'an Guo, Jie Wu*, Hongwei Hou*, Yaoting Fan

Two high-connected trinuclear Mn(II)-clusters polymers have been successfully fabricated. **1** and **2** possess high thermal stability and extraordinary chemical resistance to boiling water and familiar organic solvents. Their $\chi_M T$-T, χ_M^{-1}-T, *M(H)* and FC-ZFC measurements as well as the AC susceptibility measurements have been detailedly inquiried and deeply discussed. Strikingly, the FC and ZFC data of **1** embodies the divergence over the temperature range 40−3.5 K. **2** features the ferrimagnetic chain of a (5/2, 10/2) spin topology.